Accepted to ApJ Letters: 2012 September 28
Preprint typeset using LaTeX style emulateapj v. 5/2/11

THE MASSIVE DISTANT CLUSTERS OF WISE SURVEY: THE FIRST DISTANT GALAXY CLUSTER DISCOVERED BY WISE

Daniel P. Gettings[1], Anthony H. Gonzalez[1], S. Adam Stanford[2,3], Peter R. M. Eisenhardt[4], Mark Brodwin[5], Conor Mancone[1], Daniel Stern[4], Gregory R. Zeimann[3], Frank J. Masci[6], Casey Papovich[7], Ichi Tanaka[8], Edward L. Wright[9]

Accepted to ApJ Letters: *2012 September 28*

ABSTRACT

We present spectroscopic confirmation of a $z = 0.99$ galaxy cluster discovered using data from the Wide-field Infrared Survey Explorer (WISE). This is the first $z \sim 1$ cluster candidate from the Massive Distant Clusters of WISE Survey (MaDCoWS) to be confirmed. It was selected as an overdensity of probable $z \gtrsim 1$ sources using a combination of WISE and SDSS-DR8 photometric catalogs. Deeper follow-up imaging data from Subaru and WIYN reveal the cluster to be a rich system of galaxies, and multi-object spectroscopic observations from Keck confirm five cluster members at $z = 0.99$. The detection and confirmation of this cluster represents a first step towards constructing a uniformly-selected sample of distant, high-mass galaxy clusters over the full extragalactic sky using WISE data.

Subject headings: galaxies: clusters: individual (MOO J2342.0+1301) — galaxies: distances and redshifts — galaxies: evolution

1. INTRODUCTION

Historically, clusters of galaxies have been used as powerful probes of cosmology and galaxy evolution, providing such landmark results as the first evidence for the existence of dark matter (Zwicky 1937), demonstration of the importance of environment in galaxy evolution (Dressler 1980), and direct proof of the existence of dark matter (Clowe et al. 2004, 2006; Bradač et al. 2006). The unique leverage provided by galaxy clusters comes primarily from their extreme mass ($M > 10^{14}$ M$_\odot$) and late-time growth that continues up to the present epoch.

Large-area surveys afford the opportunity to identify well-defined samples of the most massive, rarest galaxy clusters. The ROSAT All-Sky Survey, for example, has yielded several notable catalogs of massive X-ray selected galaxy clusters to moderate redshifts (e.g. BCS at $z < 0.3$ and MACS at $z < 0.7$; Ebeling et al. 1998, 2001), while the Sloan Digital Sky Survey (SDSS) has produced large catalogs of nearby clusters covering a wider range of cluster masses (e.g. Koester et al. 2007, $0.1 < z < 0.3$). The Planck mission also provides an all-sky catalog of very massive galaxy clusters at $z < 1$ (Planck Collaboration et al. 2011a,b), while the South Pole Telescope (SPT) and Atacama Cosmology Telescope (ACT) provide complementary samples of high-mass clusters reaching to $z > 1$ for several thousand square degrees (Williamson et al. 2011; Marriage et al. 2011; Reichardt et al. 2012). However, there currently exist no surveys capable of identifying massive clusters at $z \gtrsim 1$ over the full extragalactic sky.

The most massive clusters in this redshift regime are of particular interest given the recent vigorous debate about whether the few known massive clusters at $z > 1$ are consistent with Gaussian primordial density fluctuations (Cayón et al. 2011; Hoyle et al. 2011; Enqvist et al. 2011; Williamson et al. 2011; Jee et al. 2011; Hotchkiss 2011), but a definitive answer remains elusive due to small number statistics. Moreover, the recent discovery of strong lensing by a galaxy cluster at $z = 1.75$ (Stanford et al. 2012; Brodwin et al. 2012; Gonzalez et al. 2012) revives the question of whether the frequency of giant arcs behind clusters at high redshift is consistent with ΛCDM, a question which can only be comprehensively-addressed with a statistical sample of massive clusters in this regime.

The various wavelength regimes and selection techniques used to construct galaxy cluster samples each offer unique advantages and disadvantages. Catalogs selected using the Sunyaev-Zel'dovich (SZ) effect provide high purity samples that are nearly mass-limited due to the detection signal's weak redshift dependence. These features make SZ surveys ideal for cosmological tests based upon evolution of the cluster mass function. However, the current generation of SZ catalogs are limited to $z \lesssim 1.3$, and at $z > 1$ to $M_{200} \gtrsim 3 \times 10^{14}$ M$_\odot$ and a few thousand square degrees (e.g. Marriage et al. 2011; Reichardt et al. 2012). Similar to the SZ, surveys at X-ray wavelengths provide an estimate of cluster mass immediately from detection. Current X-ray surveys are able to probe further down the mass function at high-redshift. Recent searches with XMM-Newton have proven sensitive to clusters out

[1] Department of Astronomy, University of Florida, 211 Bryant Space Center, Gainesville, FL 32611
[2] Institute of Geophysics and Planetary Physics, Lawrence Livermore National Laboratory, Livermore, CA 94550
[3] Department of Physics, University of California, One Shields Avenue, Davis, CA 95616
[4] Jet Propulsion Laboratory, California Institute of Technology, Pasadena, CA 91109
[5] Department of Physics and Astronomy, University of Missouri, 5110 Rockhill Road, Kansas City, MO 64110
[6] Infrared Processing and Analysis Center, Caltech 100-22, Pasadena, CA 91125
[7] George P. and Cynthia Woods Mitchell Institute for Fundamental Physics and Astronomy, and Department of Physics and Astronomy, Texas A&M University, College Station, TX, 77843-4242, USA
[8] Subaru Telescope, National Astronomical Observatory of Japan, 650 North A'ohoku Place, Hilo, HI 96720
[9] UCLA Astronomy, P.O. Box 951547, Los Angeles, CA 90095-1547

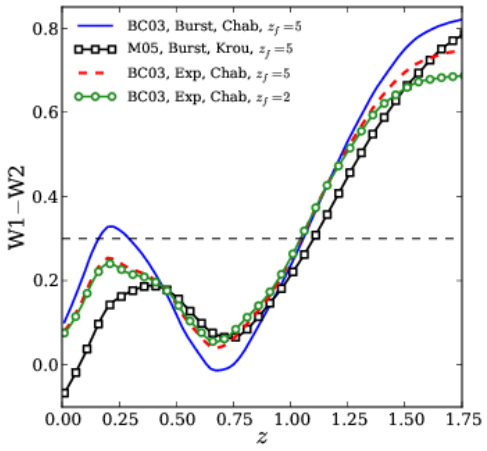

FIG. 1.— WISE W1−W2 vs. z for various simulated stellar populations. "Burst" models passively evolve after a single starburst lasting 0.1 Gyr. "Exp" models have a star formation history of the form $e^{-t/\tau}$ with $\tau = 10$ Gyr. Models labeled "BC03" come from Bruzual & Charlot (2003) and have a Chabrier (2003) initial mass function, while those labeled "M05" come from Maraston (2005) and have a Kroupa (2001) initial mass function. The formation redshift is given by z_f. The dashed horizontal line denotes the W1−W2 cut value used to select MOO J2342.0+1301. Models were generated using the EzGal package (Mancone & Gonzalez 2012).

to $z \gtrsim 1.6$ for systems with $M_{200} \gtrsim 10^{14}$ M$_\odot$ (Finoguenov et al. 2007; Papovich et al. 2010; Tanaka et al. 2010; Fassbender et al. 2011). The key factor limiting the current X-ray surveys is the area surveyed, roughly an order of magnitude less than the SZ programs. Complementary to the SZ and X-ray surveys, cluster searches with *Spitzer* based upon detecting galaxy overdensities have, in recent years, provided the greatest reach in redshift and mass sensitivity at high-redshift, extending to $z > 2$ and $M \simeq 5 \times 10^{13}$ M$_\odot$ (e.g. Eisenhardt et al. 2008; Gobat et al. 2011; Stanford et al. 2012; Zeimann et al. 2012).

The Wide-field Infrared Survey Explorer mission (WISE; Wright et al. 2010), which covers the full sky at 3.4, 4.6, 12, and 22 μm, offers the potential to find massive clusters at $z > 1$ over the full extragalactic sky. In this paper we present the first distant galaxy cluster discovered using WISE data, MOO J2342.0+1301 at $z = 0.99$. The discovery of MOO J2342.0+1301 represents a first step towards constructing an all-sky sample at $1 \lesssim z \lesssim 1.4$ as part of the Massive Distant Clusters of WISE Survey (MaDCoWS). [10]

2. WISE SELECTION OF CLUSTER CANDIDATES

2.1. *WISE Data*

The key aspect of the WISE mission enabling detection of high redshift galaxy clusters is the excellent photometric sensitivity at 3.4 and 4.6 μm (W1 and W2, respectively). The WISE All-Sky Data Release achieves 5σ sensitivity limits better than 0.07 and 0.1 mJy in unconfused regions in W1 and W2.[11] These sensitivities correspond to areas near the ecliptic plane and represent the typical minimum depth for the All-Sky survey. The effective exposure time of the observations vary significantly with ecliptic latitude due to the survey design, increasing from twelve 7.7s W1 exposures at the ecliptic plane to more than a hundred near the ecliptic poles. The WISE All-Sky Source Catalog is based on this imaging data tiled into 18,240 Atlas Images of ~ 2.4 deg^2, from which approximately 5.6×10^8 sources were extracted at a 5σ detection threshold. The WISE All-Sky Release data products, including both the Source Catalog and Image Atlas, became public on 2012 March 14 and can be accessed via the NASA/IPAC Infrared Science Archive.[12]

2.2. *Sample Definition*

Full details of the MaDCoWS galaxy cluster search method will be presented in a future paper, but we provide an overview of the essential features here. The search method that selected MOO J2342.0+1301 was based on the W1−W2 color, following the approach of Papovich (2008), who discovered a $z = 1.62$ galaxy cluster using *Spitzer*/IRAC data (Papovich et al. 2010). This method takes advantage of the fact that galaxy colors in the observed-frame $3 - 5$ μm regime become monotonically-redder between $0.75 \lesssim z \lesssim 1.75$, and are largely insensitive to variations in star formation history (see Figure 1).

After cleaning the WISE catalog of flagged sources and compensating for spatial variations in depth, in the northern hemisphere we matched the WISE extractions to the SDSS-DR8 photometric catalog (Aihara et al. 2011). For the preliminary search used to identify MOO J2342.0+1301, we then rejected sources using a combination of color and optical magnitude cuts, excluding all objects for which W1−W2 < 0.3, $i-$W1 < 5, or $i < 21$. These cuts effectively remove the bulk of the foreground galaxy population at $z < 1$. The remaining sources, consisting predominantly of high-redshift galaxies, were then binned into $\sim 10^\circ \times 10^\circ$ overlapping 2-dimensional density maps with a resolution of $15''$ pix^{-1}. These maps were smoothed with a Gaussian-difference wavelet kernel tuned to enhance structures on scales of $\sim 3'$, corresponding to a physical size of ~ 1.4 Mpc at $z \sim 1$. From these maps we identified the most statistically significant overdensities for further investigation. MOO J2342.0+1301 was selected from $\sim 10,000$ deg^2 of WISE/SDSS-DR8 overlap and was ranked very highly by both raw overdensity and visual assessments by the MaDCoWS team. Figure 2 shows the cluster in the four WISE bands, centered on the location of the brightest pixel in the associated wavelet map peak.

3. FOLLOW-UP OBSERVATIONS

3.1. *Subaru Imaging*

As part of the MaDCoWS follow-up program, MOO J2342.0+1301 was imaged using MOIRCS (Ichikawa et al. 2006; Suzuki et al. 2008) on Subaru in J and K_s on UT 2011 September 18 and 19, respectively. A total of 20 minutes of integration time was obtained in both bands, with J observed in clear conditions and $0\farcs6$ seeing and K_s observed in slightly hazy conditions with $0\farcs8$ seeing.

[10] Sources in the MaDCoWS catalog are designated as MaDCoWS Overdense Objects, which is the origin of the MOO target designation.

[11] http://wise2.ipac.caltech.edu/docs/release/allsky/expsup/sec6_3a.html

[12] http://wise2.ipac.caltech.edu/docs/release/allsky

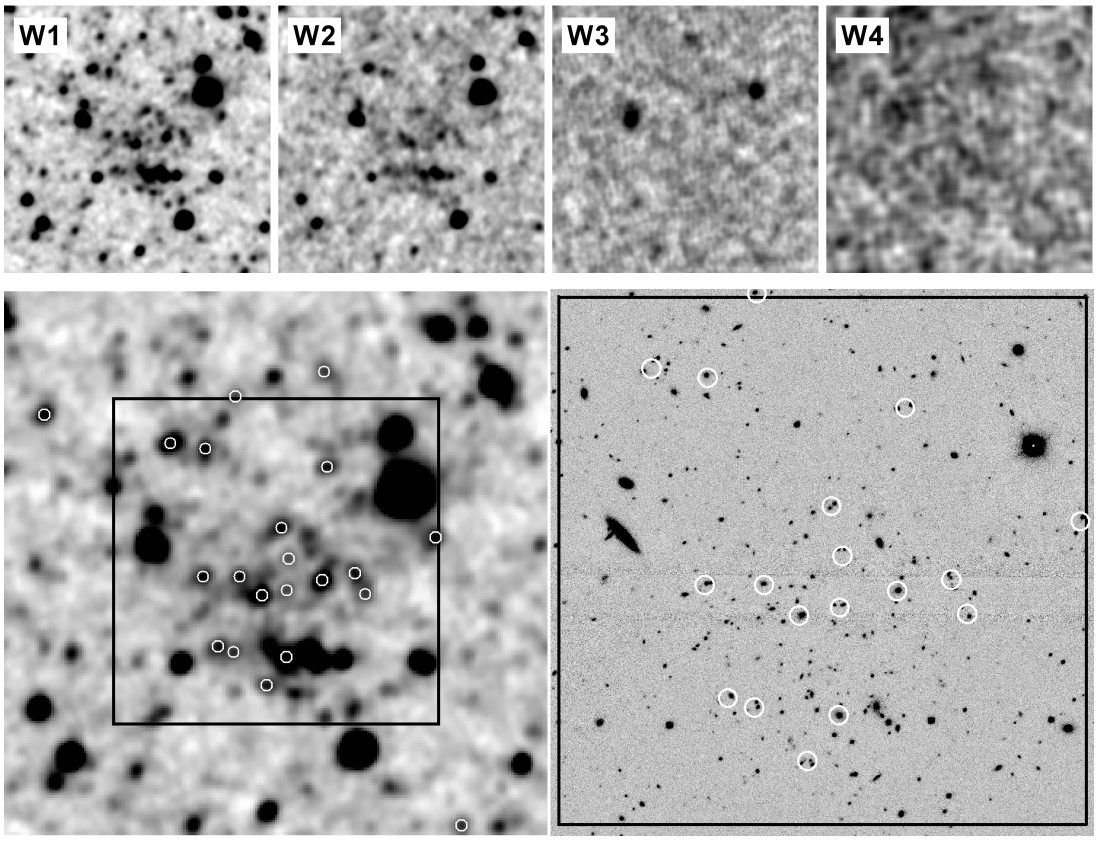

FIG. 2.— *Top:* $5' \times 5'$ images in the four WISE bands, centered at 23h42m05.6s +13d01m29s. The cluster center is taken from the brightest pixel in its associated wavelet map peak. *Bottom Left:* $5' \times 5'$ WISE-W1 image of MOO J2342.0+1301. The white circles represent sources identified as probable high-redshift galaxies based upon color and magnitude cuts (see text). The circles have a diameter of $6.1''$, comparable to the full width half at maximum of the WISE bands W1 and W2 point spread function. The box denotes a $3' \times 3'$ region centered on the detection position. *Bottom Right:* Subaru-MOIRCS K_s image of MOO J2342.0+1301. The box and circles are identical to those in the left panel. Many of the sources in the WISE imaging are blends which resolve into multiple galaxies in the deeper follow-up imaging.

The MOIRCS data were reduced using a set of IRAF scripts developed by one of the authors (Tanaka et al. 2011). The reduction procedure follows the standard methodology for the reduction of IR imaging of faint sources. After flat fielding, sky subtraction, and cosmic ray removal, the individual frames were corrected to remove geometric distortions, using a solution provided by the Subaru Observatory. These corrected frames were then registered and coadded for each detector and filter. Astrometric calibration and mosaicing of the chips were performed using the SCAMP (Bertin 2006) and SWarp (Bertin et al. 2002) software packages, using the Two Micron All Sky Survey as the astrometric reference frame (2MASS; Skrutskie et al. 2006). The data were also photometrically calibrated using 2MASS. The K_s image is shown in Figure 2.

3.2. *WIYN Imaging*

We obtained Sloan i-band imaging from the Mini-Mosaic instrument (Saha et al. 2000) on WIYN during the night of UT 2011 November 18. A total of 60 minutes of exposure was obtained in $0\farcs9$ seeing using three dithered 20 minute integrations. The data were processed using standard reduction procedures in IRAF and astrometrically calibrated to the USNO-B1.0 catalog (Monet et al. 2003) using SCAMP and SWarp. Photometric calibration of final, stacked images was performed using SDSS-DR8 stars in the field. A color composite of the i, J and K_s images is shown in Figure 3.

3.3. *Keck Spectroscopy*

Based on the Subaru imaging results, a slit-mask was designed to be used with the Low-Resolution Imaging Spectrometer (LRIS; Oke et al. 1995) at the Keck Observatory to obtain redshifts of potential cluster galaxies. Sources for the mask were selected using $J - K_s$ colors, K_s magnitudes, and distance from the nominal cluster center, with final selection also accounting for slit-positioning constraints. Spectra were obtained on UT 2011 October 22 using $1\farcs1 \times 10''$ slitlets, the G400/8500 grating on the red side, the D680 dichroic, and G300/5000 grism on the blue side. Four 1200 s exposures were obtained in mostly clear conditions with $0\farcs6$ seeing.

The LRIS spectra were split into slitlets which were separately reduced using standard long-slit procedures in IRAF. The relative spectral response was calibrated via longslit observations of Wolf 1346 and Hiltner 600. Redshifts were determined by visual inspection using prominent spectral features including the 4000 Angstrom break, the Ca H+K absorption lines, and the [O II] λ3727 emission line.

4. RESULTS

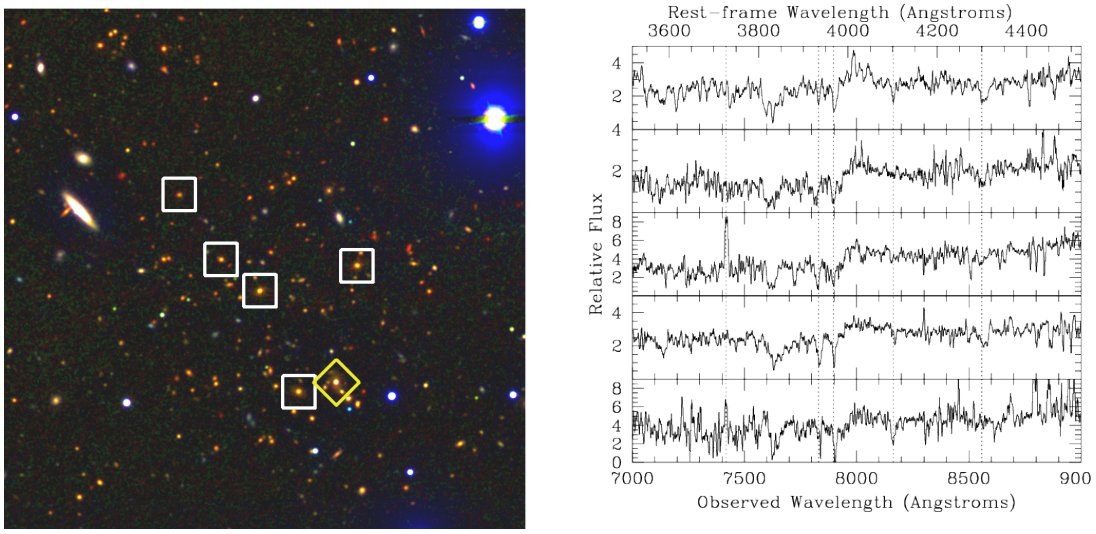

FIG. 3.— *Left:* A WIYN-i and Subaru JK_s 3-color image of the central $3' \times 3'$ region of MOO J2342.0+1301. Boxes indicate spectroscopically confirmed cluster members. The diamond denotes an object with a redshift that is not at the cluster redshift. Of the six galaxies targeted in the LRIS mask which are within 500 kpc of the nominal cluster center, five were confirmed to be cluster members. *Right:* LRIS spectra of the five member galaxies. The rest-frame wavelength at $z = 0.99$ is shown along the top. The vertical dotted lines mark the positions of the following features (from left to right): [O II]λ3727, Ca H+K, Hδ, and the G-band.

4.1. *Redshifts*

The Keck spectroscopy yielded high-quality redshifts for 12 galaxies. Geometrical constraints on the slit placement allowed observations of only six galaxies within a projected distance of 500 kpc from the nominal cluster center. Five were confirmed to be cluster members, with redshifts lying within $\Delta z = 0.010$, or ± 750 km s^{-1}, of $z = 0.987$, the mean cluster redshift. In Table 1 we provide coordinates, redshifts, identifying features, and a quality assessment for each redshift. All but one of the confirmed cluster members were identified based only on absorption lines and continuum breaks, rather than emission lines, a feature characteristic of the members of mature galaxy clusters. The spectra of the five confirmed cluster members are shown in Figure 3.

4.2. *Color–Magnitude Diagram*

We use imaging data from Subaru and WIYN to construct the $J - K_s$ color-magnitude diagram (CMD) for MOO J2342.0+1301. Photometry was obtained using SExtractor version 2.5.0 (Bertin & Arnouts 1996) in dual-image mode with K_s used for source detection. We present the resulting CMD in Figure 4. Light grey diamonds show all galaxies within a projected 500 kpc radius of the cluster center that have $i - J > 1.38$, the color given by a Bruzual & Charlot (2003) exponential model with $\tau = 10$ Gyr, formed at $z_f = 5$ and observed at $z = 0.99$. Spectroscopically confirmed members and non-members are marked with black boxes (red in the online version) and black crosses, respectively. Additionally, we denote with large circles (blue in the online version) all K_s-selected objects that lie within the footprint of the $\sim$6.1″ WISE PSF for each WISE source that satisfies the color and magnitude cuts described in Section 2.2 (see also Figure 2). It is these WISE sources, the majority of which are composed of multiple blended components, that contributed to the detection signal for the cluster. We include lines showing the expected $J - K_s$ color (horizontal) and apparent K_s magnitude (vertical) of an L^* galaxy at $z = 0.99$, using a Bruzual & Charlot (2003) simple stellar population model with solar metallicity and a Chabrier (2003) initial mass function, formed at $z_f = 5$. The red sequence in this cluster is well-populated, with both the spectroscopic members and galaxies corresponding to the WISE sources contributing to detection of the cluster lying near the expected $z = 0.99$ color.

5. DISCUSSION

The discovery of MOO J2342.0+1301 represents the first result from MaDCoWS, whose goal is to conduct a wide-area search for such massive clusters at $1 \lesssim z \lesssim 1.4$. This program is designed to be complementary to previous, shallower all-sky cluster surveys, enabling future investigations of the most extreme clusters at this epoch. Forthcoming papers will present details for the full MaDCoWS program, including the ongoing followup program and characterization of the cluster selection function.

Finally, we note that this cluster was found using the WISE All-Sky Data Release, which includes only data obtained during the cryogenic mission. Data continued to be collected at 3.4 μm and 4.6 μm after exhaustion of the WISE cryogen supply as part of the NEOWISE (Mainzer et al. 2011) survey of the asteroid belt. However, the asteroid search required only that individual exposures be processed, so the multiple observations of inertially fixed sources from this phase of the mission have not been combined. Fully processing and combining this post-cryogenic data with the cryogenic data in these bands, which has now been funded by NASA, would double the all-sky coverage from WISE in W1 and W2, improving the fidelity and redshift reach of WISE for discovering the most massive, distant galaxy clusters.

The authors thank the anonymous referee whose comments improved the quality of the manuscript. This

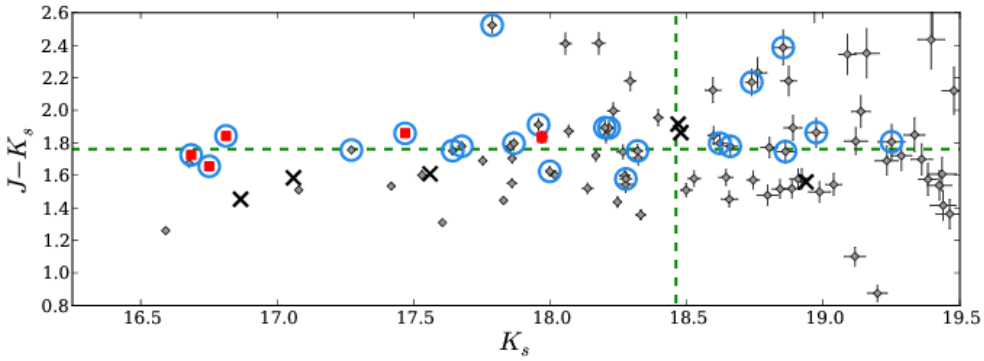

FIG. 4.— $(J - K_s)$ vs. K_s color-magnitude diagram for MOO J2342.0+1301. Gray diamonds denote galaxies that lie within a 500 kpc projected radius of the cluster center with $i - J > 1.38$. Black squares (red in the online version) are spectroscopically confirmed cluster members. Black "X" points represent non-member galaxies with spectroscopic redshifts. Large circles (blue in the online version) indicate all objects found within 3.05″ of the WISE sources that contributed to the detection signal (see Figure 2). The vertical and horizontal dashed lines show the expected K_s magnitude and $J-K_s$ color for an L^* galaxy formed at $z_f = 5$ and observed at $z = 0.99$. All magnitudes are on the Vega system.

TABLE 1
SPECTROSCOPIC RESULTS

α (J2000)	δ (J2000)	J	K_s	z	Quality	Features
			Members			
23:42:04.80	+13:00:50.0	18.40	16.75	0.989	A	[O II], D4000, Ca H+K
23:42:03.43	+13:01:32.7	18.66	16.81	0.993	B	D4000, Ca H+K
23:42:05.67	+13:01:24.2	18.37	16.69	0.983	A	D4000, Ca H+K
23:42:06.57	+13:01:34.9	19.33	17.47	0.987	B	D4000, Ca H+K
23:42:07.56	+13:01:56.8	19.81	17.97	0.985	A	D4000, Hδ
			Non-Members			
23:42:03.93	+13:00:53.2	17.65	16.00	0.784	B	Ca H+K
23:41:57.98	+13:00:51.0	19.17	17.56	1.043	B	[O II]
23:41:58.15	+12:59:17.1	18.66	17.06	0.777	A	Ca H+K, D4000
23:42:08.86	+13:02:47.9	20.38	18.47	1.210	B	D4000
23:41:59.87	+12:59:14.9	20.47	18.94	1.172	A	[O II]
23:41:59.28	+12:58:09.6	20.34	18.48	0.622	A	[O II], Hβ
23:42:00.65	+12:58:16.2	18.33	16.87	0.249	A	Hα, [S II]

NOTE. — Coordinates, redshifts, identifying features, and quality assessments of each redshift obtained from LRIS observations on Keck I. The typical redshift uncertainty is $\delta z \simeq 0.001$. Quality flag "A" signifies a robust redshift determination, typically relying upon multiple emission or absorption features. Quality flag "B" signifies a redshift determination that is less certain, but still unambiguous with at least two features. Magnitudes are on the Vega system.

publication makes use of data products from the Wide-field Infrared Survey Explorer, which is a joint project of the University of California, Los Angeles and the Jet Propulsion Laboratory/California Institute of Technology, funded by the National Aeronautics and Space Administration (NASA). D. P. G. and A. H. G. acknowledge support for this research from the NASA Astrophysics Data Analysis Program (ADAP) through grant NNX12AE15G. Some of the data presented herein were obtained at the W.M. Keck Observatory, which is operated as a scientific partnership among the California Institute of Technology, the University of California and the National Aeronautics and Space Administration. The Observatory was made possible by the generous financial support of the W.M. Keck Foundation. Based in part on data collected at Subaru Telescope, which is operated by the National Astronomical Observatory of Japan. D. P. G. was a Visiting Astronomer, Kitt Peak National Observatory, National Optical Astronomy Observatory, which is operated by the Association of Universities for Research in Astronomy (AURA) under cooperative agreement with the National Science Foundation. The WIYN Observatory is a joint facility of the University of Wisconsin-Madison, Indiana University, Yale University, and the National Optical Astronomy Observatory. This research has made use of the NASA/ IPAC Infrared Science Archive, which is operated by the Jet Propulsion Laboratory, California Institute of Technology, under contract with the National Aeronautics and Space Administration.

REFERENCES

Aihara, H., Allende Prieto, C., An, D., et al. 2011, ApJS, 193, 29
Bertin, E. 2006, in Astronomical Society of the Pacific Conference Series, Vol. 351, Astronomical Data Analysis Software and Systems XV, ed. C. Gabriel, C. Arviset, D. Ponz, & S. Enrique, 112
Bertin, E., & Arnouts, S. 1996, A&AS, 117, 393
Bertin, E., Mellier, Y., Radovich, M., et al. 2002, in Astronomical Society of the Pacific Conference Series, Vol. 281, Astronomical Data Analysis Software and Systems XI, ed. D. A. Bohlender, D. Durand, & T. H. Handley, 228
Bradač, M., Clowe, D., Gonzalez, A. H., et al. 2006, ApJ, 652, 937
Brodwin, M., Gonzalez, A. H., Stanford, S. A., et al. 2012, ApJ, 753, 162
Bruzual, G., & Charlot, S. 2003, MNRAS, 344, 1000
Cayón, L., Gordon, C., & Silk, J. 2011, MNRAS, 415, 849
Chabrier, G. 2003, PASP, 115, 763
Clowe, D., Bradač, M., Gonzalez, A. H., et al. 2006, ApJ, 648, L109
Clowe, D., Gonzalez, A., & Markevitch, M. 2004, ApJ, 604, 596
Dressler, A. 1980, ApJ, 236, 351
Ebeling, H., Edge, A. C., Bohringer, H., et al. 1998, MNRAS, 301, 881
Ebeling, H., Edge, A. C., & Henry, J. P. 2001, ApJ, 553, 668
Eisenhardt, P. R. M., Brodwin, M., Gonzalez, A. H., et al. 2008, ApJ, 684, 905
Enqvist, K., Hotchkiss, S., & Taanila, O. 2011, **??**jnlJ. Cosmology Astropart. Phys., 4, 17
Fassbender, R., Böhringer, H., Nastasi, A., et al. 2011, New Journal of Physics, 13, 125014
Finoguenov, A., Guzzo, L., Hasinger, G., et al. 2007, ApJS, 172, 182
Gobat, R., Daddi, E., Onodera, M., et al. 2011, A&A, 526, A133
Gonzalez, A. H., Stanford, S. A., Brodwin, M., et al. 2012, ApJ, 753, 163
Hotchkiss, S. 2011, JCAP, 7, 4
Hoyle, B., Jimenez, R., & Verde, L. 2011, Phys. Rev. D, 83, 103502
Ichikawa, T., Suzuki, R., Tokoku, C., et al. 2006, in Society of Photo-Optical Instrumentation Engineers (SPIE) Conference Series, Vol. 6269, Society of Photo-Optical Instrumentation Engineers (SPIE) Conference Series
Jee, M. J., Dawson, K. S., Hoekstra, H., et al. 2011, ApJ, 737, 59
Koester, B. P., McKay, T. A., Annis, J., et al. 2007, ApJ, 660, 239
Kroupa, P. 2001, MNRAS, 322, 231
Mainzer, A., Bauer, J., Grav, T., et al. 2011, ApJ, 731, 53
Mancone, C. L., & Gonzalez, A. H. 2012, PASP, 124, 606
Maraston, C. 2005, MNRAS, 362, 799
Marriage, T. A., Acquaviva, V., Ade, P. A. R., et al. 2011, ApJ, 737, 61
Monet, D. G., Levine, S. E., Canzian, B., et al. 2003, AJ, 125, 984
Oke, J. B., Cohen, J. G., Carr, M., et al. 1995, PASP, 107, 375
Papovich, C. 2008, ApJ, 676, 206
Papovich, C., Momcheva, I., Willmer, C. N. A., et al. 2010, ApJ, 716, 1503
Planck Collaboration, Ade, P. A. R., Aghanim, N., et al. 2011a, A&A, 536, A8
Planck Collaboration, Aghanim, N., Arnaud, M., et al. 2011b, A&A, 536, A26
Reichardt, C. L., Stalder, B., Bleem, L. E., et al. 2012, ArXiv e-prints
Saha, A., Armandroff, T., Sawyer, D. G., & Corson, C. 2000, in Society of Photo-Optical Instrumentation Engineers (SPIE) Conference Series, Vol. 4008, Society of Photo-Optical Instrumentation Engineers (SPIE) Conference Series, ed. M. Iye & A. F. Moorwood, 447–451
Skrutskie, M. F., Cutri, R. M., Stiening, R., et al. 2006, AJ, 131, 1163
Stanford, S. A., Brodwin, M., Gonzalez, A. H., et al. 2012, ApJ, 753, 164
Suzuki, R., Tokoku, C., Ichikawa, T., et al. 2008, PASJ, 60, 1347
Tanaka, I., Breuck, C. D., Kurk, J. D., et al. 2011, PASJ, 63, 415
Tanaka, M., Finoguenov, A., & Ueda, Y. 2010, ApJ, 716, L152
Williamson, R., Benson, B. A., High, F. W., et al. 2011, ApJ, 738, 139
Wright, E. L., Eisenhardt, P. R. M., Mainzer, A. K., et al. 2010, AJ, 140, 1868
Zeimann, G. R., Stanford, S. A., Brodwin, M., et al. 2012, ApJ, 756, 115
Zwicky, F. 1937, ApJ, 86, 217